Acta Crystallographica Section D
Biological Crystallography
ISSN 0907-4449

The structure of S100A12 in a hexameric form and its proposed role in receptor signalling

O. V. Moroz,[a] A. A. Antson,[a] E. J. Dodson,[a] H. J. Burrell,[a] S. J. Grist,[a] R. M. Lloyd,[a] N. J. Maitland,[b] G. G. Dodson,[a,c] K. S. Wilson,[a] E. Lukanidin[d] and I. B. Bronstein[a]*

[a]Department of Chemistry, University of York, York YO10 5DD, England, [b]Yorkshire Cancer Research Unit, Department of Biology, University of York, York YO10 5DD, England, [c]National Institute of Medical Research, Mill Hill, London NW7 1AA, England, and [d]Department of Molecular Cancer Biology, Institute for Cancer Biology, Danish Cancer Society, Strandboulevarden 49, Copenhagen 2100, Denmark

Correspondence e-mail: igor@ysbl.york.ac.uk

Received 3 October 2001
Accepted 11 December 2001

PDB Reference: S100A12 hexameric form, 1gqm, r1gqmsf.

S100A12 is a member of the S100 subfamily of EF-hand calcium-binding proteins; it has been shown to be one of the ligands of the 'receptor for advanced glycation end products' (RAGE) that belongs to the immunoglobulin superfamily and is involved in diabetes, Alzheimer's disease, inflammation and tumour invasion. The structure of the dimeric form of native S100A12 from human granulocytes in the presence of calcium in space group $R3$ has previously been reported. Here, the structure of a second crystal form in space group $P2_1$ (unit-cell parameters $a = 53.9$, $b = 100.5$, $c = 112.7$ Å, $\beta = 94.6^\circ$) solved at 2.7 Å resolution by molecular replacement using the $R3$ structure as a search model is reported. Like most S100 proteins, S100A12 is a dimer. However, in the $P2_1$ crystal form dimers of S100A12 are arranged in a spherical hexameric assembly with an external diameter of about 55 Å stabilized by calcium ions bound between adjacent dimers. The putative target-binding sites of S100A12 are located at the outer surface of the hexamer, making it possible for the hexamer to bind several targets. It is proposed that the S100A12 hexameric assembly might interact with three extracellular domains of the receptor, bringing them together into large trimeric assemblies.

1. Introduction

The S100 protein family is made up of calcium-modulated proteins of the EF-hand type with diverse functional roles in cell differentiation and migration (reviewed in Donato, 2001; Heizmann & Cox, 1998; Schäfer & Heizmann, 1996; Kligman & Hilt, 1988). Most S100 family members were isolated from cells in the form of dimers. The dimers have two target-binding sites, with both subunits contributing to each of them. The target-binding sites are located on opposite sides of the dimer, creating the possibility that S100 proteins might functionally cross-bridge two similar or even different target proteins. S100 proteins have both intracellular and extracellular functions. The mechanism of secretion of S100 proteins is still unclear, but the first data have started to emerge. Recent reports on S100A13 show that it is released in a Cu^{2+}-dependent complex with fibroblast growth factor 1 (Landriscina, Bagala *et al.*, 2001; Landriscina, Soldi *et al.*, 2001). Similar secretion mechanisms could work for other S100 proteins. There is increasing evidence that secreted S100 proteins are able to form oligomers (Réty *et al.*, 1999; Strupat *et al.*, 2000). Moreover, it has been shown that S100A4 oligomers have enhanced biological activity in stimulating angiogenesis (Ambartsumian *et al.*, 2001) and neurite outgrowth (Novitskaya *et al.*, 2000).

Human S100A12 is a member of the calgranulin subfamily (Guignard *et al.*, 1995). It is expressed exclusively in

granulocytes (Vogl *et al.*, 1999), while two other calgranulins S100A8 and S100A9 are more widely expressed. Recent data indicate that while the two other calgranulins interact with each other, forming heterodimers and heterotetramers (Strupat *et al.*, 2000), S100A12 does not interact with either S100A8 or A9 or the A8/A9 complex (Vogl *et al.*, 1999). It therefore probably plays a different role in calcium-induced signalling (Robinson & Hogg, 2000). Human S100A12 has 70% sequence identity with both pig (Dell'Angelica *et al.*, 1994; Nonato *et al.*, 1997) and rabbit S100A12 (Yan *et al.*, 1996) and 78% with the bovine (Hitomi *et al.*, 1996) protein.

It is very likely that S100A12, as well as some other S100 proteins, belongs to a new class of chemokines and contributes to cell migration (Miranda *et al.*, 2001). Involvement of S100A12 in chronic inflammatory responses has been reported: for example, during human onchocerciasis (Marti *et al.*, 1996), in monocyte migration and in rheumatoid arthritis (Yang *et al.*, 2001).

In addition to the calcium sites, a single Zn^{2+}-binding site per monomer was identified in pig S100A12 by means of fluorimetric titration (Dell'Angelica *et al.*, 1994). Following this, sequence analysis of human and pig S100A12 as well as human S100A8 and A9 showed the presence of an H*xxx*H Zn-binding motif close to the C-terminus (Marti *et al.*, 1996). The Zn-binding site was more fully characterized from the three-dimensional structure of the homologous S100A7 zinc complex (Brodersen *et al.*, 1999) and was shown to contain an additional His and a Glu from the N-terminus. Furthermore, there is evidence that some S100 family members can also bind copper and that Zn^{2+} and Cu^{2+} share the same binding site (Nishikawa *et al.*, 1997; Heizmann & Cox, 1998), although for S100A5 it was alternatively suggested that copper might substitute Ca^{2+} in the EF-hands (Schäfer *et al.*, 2000).

A cell-surface receptor for S100A12, the 'receptor for advanced glycation end products' (RAGE), has been identified on endothelium, inflammatory cells and neurons. Interaction of RAGE with S100A12 mediates a novel pro-inflammatory axis (Hofmann *et al.*, 1999). RAGE is a member of the immunoglobulin superfamily of cell-surface receptors (Springer, 1990; Harpaz & Chothia, 1994). It had first been discovered as the receptor for the advanced glycation end products that form at an accelerated rate in diabetes (Neeper *et al.*, 1992). Increased expression of RAGE in Alzheimer's disease brain tissue indicates that it is relevant to the pathogenesis of neuronal disfunction and death (Yan *et al.*, 1996). RAGE binds amphoterin and mediates neurite outgrowth (Huttunen *et al.*, 1999), while blockage of RAGE–amphoterin signalling decreases tumour growth and metastases (Taguchi *et al.*, 2000).

The immunoglobulin superfamily of receptors is closely related to the cytokine receptor superfamily; they are both thought to be derived from the same ancestor: a primitive cell-adhesion molecule (Bazan, 1990). There is increasing evidence of receptor oligomerization as a general mechanism for signal propagation by the cytokine family receptors (reviewed in Bravo & Heath, 2000). Receptor oligomerization is a mechanism during which an oligomeric ligand interacts with two or more receptor extracellular domains. This interaction may change the conformation of the cytoplasmic domains, thus activating intracellular signalling. For the cytokine superfamily it is usually thought to be receptor dimerization, but the X-ray studies of the human interferon-γ receptor complex revealed a third receptor molecule which is possibly functionally significant (Thiel *et al.*, 2000). In the tumour necrosis factor (TNF) receptor superfamily, receptor trimerization is now confirmed as a signalling mechanism. Signalling starts when a trimer of TNF binds to the extracellular domains of three receptor molecules (Banner *et al.*, 1993; Naismith *et al.*, 1996), which permits the aggregation and activation of three cytoplasmic domains that bind to a trimer of tumour necrosis receptor associated factor (TRAF) (Park *et al.*, 1999; McWhirter *et al.*, 1999; Ye *et al.*, 1999; Ni *et al.*, 2000; Wajant *et al.*, 2001).

We report here the structure of a S100A12 hexamer and propose a role of the hexameric assembly in RAGE-mediated signalling.

Table 1
X-ray data statistics.

Resolution (Å)	No. of unique reflections	$\langle I/\sigma(I)\rangle$	$I/\sigma(I) > 3$	Completeness (%)	$R_{\rm merge}(I)$† (%)
20.00–5.77	3269	26.4	93.9	97.0	2.4
5.77–4.60	3251	23.9	94.0	97.9	3.6
4.60–4.03	3266	22.8	94.8	98.5	3.7
4.03–3.66	3256	19.4	92.7	98.8	4.8
3.66–3.40	3252	13.4	87.4	98.9	7.0
3.40–3.20	3256	10.0	82.2	99.1	9.4
3.20–3.04	3266	6.0	65.5	99.2	11.8
3.04–2.91	3277	4.4	53.9	99.3	22.9
2.91–2.80	3246	3.3	41.6	99.1	29.8
2.80–2.70	3107	2.3	27.5	95.3	41.2
All *hkl*	32446	16.7	73.6	98.3	5.3

† $R_{\rm merge}$ is defined as $100 \times \sum |I - \langle I\rangle| / \sum I$, where I is the intensity of the reflection.

2. Methods

2.1. Crystallization and data collection

S100A12 was purified from human granulocytes as described previously (Moroz *et al.*, 2000) and crystallized by hanging-drop vapour diffusion with 4–7 mg ml^{-1} protein in a 1 µl drop and 10–20% PEG 5000 MME, 0.2 *M* $CaCl_2$ and 0.1 *M* sodium cacodylate pH 6.5 in the reservoir. Crystallization conditions were similar to those for the *R*3 crystal form. Crystals belong to the space group $P2_1$, with unit-cell parameters a = 53.9, b = 100.5, c = 112.7 Å, β = 94.6°. The crystals were characterized using Cu $K\alpha$ X-rays from a Rigaku RU-200 rotating-anode generator. There are 12 subunits of S100A12 in the asymmetric unit, resulting in a specific volume $V_{\rm M}$ of 2.43 Å^3 Da^{-1} and a solvent content of 48.9%.

Complete data were collected to 2.7 Å resolution using synchrotron radiation at the ESRF beamline 14-4 (wavelength 0.93 Å). The data were processed with *DENZO* and *SCALEPACK* (Otwinowski & Minor, 1997). 85 375 reflections were reduced to 32 446 unique observations, giving an

average redundancy of 2.6. The X-ray data statistics are summarized in Table 1.

2.2. Structure determination and refinement

Crystallographic calculations were performed using the *CCP*4 program package (Collaborative Computational Project, Number 4, 1994). The structure was solved by molecular replacement with *AMoRe* (Navaza, 1994) using the structure of the S100A12 dimer from the *R*3 crystal form as a search model. Five solutions were found. The position of the sixth dimer, which is less ordered, was confirmed using the *FFFEAR* program (Cowtan, 1998), which can search for molecular fragments in poor-quality electron-density maps. The solvent content was set to 55% and the search step to 5°. The structure was refined using *REFMAC* (Murshudov & Dodson, 1997). Initially, each monomer was treated as a rigid body. After convergence of rigid-body refinement, individual atomic refinement was conducted with NCS restraints (tight restraints for the main chain, loose restraints for the side chains). The resulting map was averaged with *MAPROT* and manual model rebuilding was performed using the XFIT (Oldfield, 1994) option of the program *QUANTA* (Molecular Simulations Inc.). For further refinement, the TLS option (Schomaker & Trueblood, 1968; Winn *et al.*, 2001) was used to account for the overall anisotropic motion of the monomers. From this stage, model rebuilding was performed individually for each subunit. The results of refinement are summarized in Table 2.

2.3. Quality of the final model

The structure of the S100A12 hexamer has been refined to an *R* factor of 21.7% for all data in the resolution range 20.0–2.7 Å, excluding the randomly distributed 3% of the reflections assigned to calculate $R_{\rm free}$ (28.1%). There are 12 monomers in the asymmetric unit, arranged as two trimers of dimers. The final electron-density map allowed the positioning of all residues except the C-terminal segments 88–91 for all subunits (87–91 for *L*), the side chains of several surface residues (mostly lysines) and the main chain for residues Gln16, Asp25, Gln34 and Thr37–Lys38 for the most poorly defined subunit *L*. The model contains 8514 atoms including 36 Ca atoms and 28 water molecules. All residues are in the allowed regions of the Ramachandran plot (Ramakrishnan & Ramachandran, 1965), with 91.6% in the most favoured regions (Fig. 1).

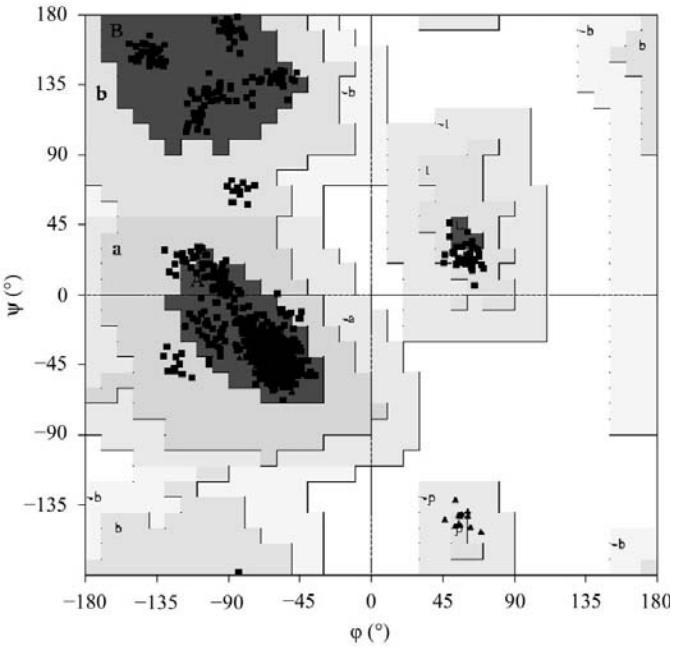

Figure 1
Ramachandran plot for the 12 subunits of S100A12 calculated using *PROCHECK* (Laskowski *et al.*, 1993).

Table 2
Model refinement statistics.

Resolution limits (Å)	20.0–2.7
Total No. of reflections	31345
Percentage observed	100
Percentage of free reflections	3
$R_{\rm cryst}$† (%)	21.7
Free *R* factor (%)	28.1
R.m.s. deviations from ideal geometry‡	
Bond distances (Å)	0.018 (0.021)
Bond angles (°)	1.861 (1.931)
Chiral centres (Å^3)	0.12 (0.20)
Planar groups (Å)	0.006 (0.020)
Main-chain bond *B* values (Å^2)	0.38 (1.50)
Main-chain angle *B* values (Å^2)	0.80 (2.00)
Side-chain bond *B* values (Å^2)	1.68 (3.00)
Side-chain angle *B* values (Å^2)	2.82 (4.50)

† $R_{\rm cryst} = \sum ||F_o| - |F_c|| / \sum |F_o|$. ‡ Target values are given in parentheses.

2.4. Dynamic light-scattering analysis

Dynamic light-scattering analysis (DLS) was carried out using a Dynapro-801 molecular-sizing instrument. A 20 µl sample with a protein concentration of 4 mg ml^{-1} was centrifuged at 14 000 rev min^{-1} for 10 min and transferred into a 20 µl chamber quartz cuvette. The data were analysed using the *Dynamics* 4.0 and *DynaLS* software (Protein Solutions).

2.5. Cloning and expression of RAGE extracellular domain

Full-size RAGE cDNA was amplified from the Marathon human lung cDNA library (Clontech) using an Advantage2 PCR kit (Clontech). A RAGE extracellular fragment bearing the putative S100-binding site was cloned into the pVL1392 vector and expressed in Sf21 insect cells using the baculovirus expression system. Expressed protein was purified on a Bio-Rex70 cation-exchange column (Bio-Rad) and a RESOURCES cation-exchange column (Pharmacia). Finally, the protein was concentrated to 0.2 mg ml^{-1} using a Filtron 10K ultrafiltration membrane.

The purification procedure for recombinant S100A12 was similar to that for S100A4 described in Tarabykina *et al.* (2001).

2.6. Far-Western blot analysis of S100A12/RAGE interaction

Purified RAGE was electrophoresed in a 4–12% bis-Tris polyacrylamide gel (Novex) in MES–Tris buffer for 40 min at 200 V and transferred onto PVDF membrane by electroblotting at 250 mA for 45 min. The membrane was incubated for 1 h at room temperature with 30 µg ml^{-1} recombinant S100A12 in blocking buffer (Boehringer–Mannheim chemiluminiscence system for detection of proteins). Bound protein was detected by incubation with rabbit polyclonal anti-S100A12 (dilution 1:5000, overnight, 277 K) and then with peroxidase-conjugated anti-rabbit IgG antibody (Bio-Rad, dilution 1:5000, 1 h at room temperature) and detected by electrogenerated chemiluminescence (Boehringer–Mannheim chemiluminiscence system for detection of proteins). Anti-S100A12 antibody was kindly provided by Dr N. Hogg (Imperial Cancer Research Fund, London).

3. Results and discussion

3.1. The S100A12 hexamer

The hexamer is arranged as a trimer of dimers, with each dimer having similar architecture and structure to that of a dimer in the *R*3 crystal form (Moroz *et al.*, 2001). The overall surface of the hexamer is 22 426 Å^2, with a total area of contact between the monomers of 6118 Å^2 and an area of contact between the dimers of 2026 Å^2. The area of contact here was defined as $S_{\rm contact} = (n \times S_{\rm mon} - S_{n\text{-mer}})/2$, where $S_{\rm mon}$ is the area of a monomer and $S_{n\text{-mer}}$ is the area of the *n*-fold oligomer. The approximate diameter of the hexamer is 55 Å; the diameter of the central hole is about 8–10 Å. The structures of the 12 crystallographically independent monomers in the asymmetric unit are essentially the same, with the significant differences mainly restricted to a few side chains. The root-mean-square deviations in the main-chain atom positions (r.m.s.$_{xyz}$) between subunit *A* and the other 11 subunits (*B*, *C*, *D*, *E*, *F*, *G*, *H*, *I*, *J*, *K*, *L*) and the average *B* factors for each chain are shown in Table 3.

Table 3
Comparison of the independent subunits.

N is the chain identification letter; r.m.s.$_{xyz}$ is the r.m.s. deviation for coordinates (Å); $B_{\rm ave}$ is the average *B* factor (Å^2).

N	*A*	*B*	*C*	*D*	*E*	*F*	*G*	*H*	*I*	*J*	*K*	*L*
R.m.s.$_{xyz}$ (*A*:*N*)	—	0.21	0.20	0.23	0.22	0.18	0.18	0.22	0.22	0.22	0.21	0.29
$B_{\rm ave}$ main chain	22.4	22.4	22.4	22.4	22.4	22.4	22.3	22.5	22.4	22.4	22.3	22.8
$B_{\rm ave}$ side chain	23.9	24.1	24.1	23.8	23.8	23.6	23.8	24.0	23.8	23.8	24.0	24.2

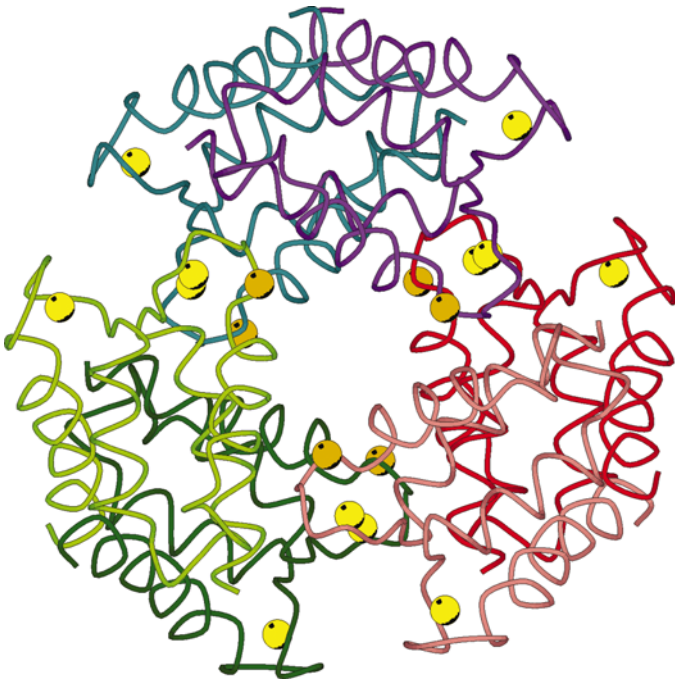

Figure 2
C_α trace of the S100A12 hexamer viewed down the non-crystallographic threefold axis. The three dimers forming the hexamer are coloured blue, red and green, with different shades for each monomer. The 'EF-hand' calciums are bright yellow and the calciums in the hexamer-forming interface are dark yellow. This figure and Fig. 4 were generated using the program *MOLSCRIPT* (Kraulis, 1991).

In the hexamer structure there is a further bound Ca^{2+} ion per monomer in addition to the two in the EF-hands. The additional calcium ions are coordinated by the residues from two adjacent dimers, and cause the dimers to associate into hexamers (Fig. 2). There is a total of six of these calcium ions per hexamer, in addition to the 12 'canonical' calciums bound to EF-hand motifs. The ability of S100A12 to bind additional calcium agrees well with the results of electrospray ionization mass-spectrometry analysis (Strupat *et al.*, 2000). We have confirmed S100A12 oligomerization in solution in the presence of calcium by DLS data, which show an increase of the hydrodynamic radius from 1.9 to 2.9 nm in the presence of 5 m*M* calcium. This would correspond to an increase in the molecular weight from 18 to 52 kDa assuming the standard settings for the molecular-weight estimate, in good agreement with the molecular weights of the S100A12 dimer (20.9 kDa) and hexamer, respectively. When the calcium concentration is increased to 200 m*M*, as in the crystallization buffer, the R_H decreased to 2.4 nm. This probably means that the dissociation of some hexamers into dimers occurs at such high calcium concentrations and explains the existence of two crystal forms under the same conditions.

The inter-dimer calcium ion is coordinated by the side-chain O atoms of Gln58 and Gln64 from the subunit of one dimer and the bidentate carboxyl group of Glu55 from another dimer (Fig. 3). The electron density in the region of the calcium-binding sites is well defined: the mean *B* value for the calcium ions is 22.5 Å^2, with the *B* values of calcium-binding O atoms varying between 20.4 and 25.3 Å^2. The average calcium coordination distances are: Gln58 OE1, 2.05 (0.13) Å; Glu55 OE1 and OE2, 2.45 (0.20) Å and 2.43 (0.22) Å, respectively; Gln64 OE1, 2.24 (0.13) Å, with the r.m.s. devia-

tions given in parentheses estimated from the experimental spread of values; this is well within the limits for calcium–oxygen distances at 2.7 Å resolution (Harding, 2001). In addition, Glu66 from the first dimer moves towards the new calcium-binding site relative to its position in the *R*3 structure. The side-chain O atoms of Glu66 are rather close to the intermolecular calcium (mean distances are 4.5 and 5.3 Å), so the calcium ion could be coordinated through an additional bridging water molecule which is not visible in the electron-density maps at this resolution. The residues involved in intramolecular calcium binding vary throughout the S100 family, suggesting that this mode of hexamer formation is a unique feature of S100A12.

Contacts through intermolecular metal-binding sites are common in hexamer formation, as seen in annexin XII where the hexamer has six intermolecular calcium-binding sites (Luecke *et al.*, 1995) or insulin which forms a hexamer by binding two or more zinc ions (Whittingham *et al.*, 1998).

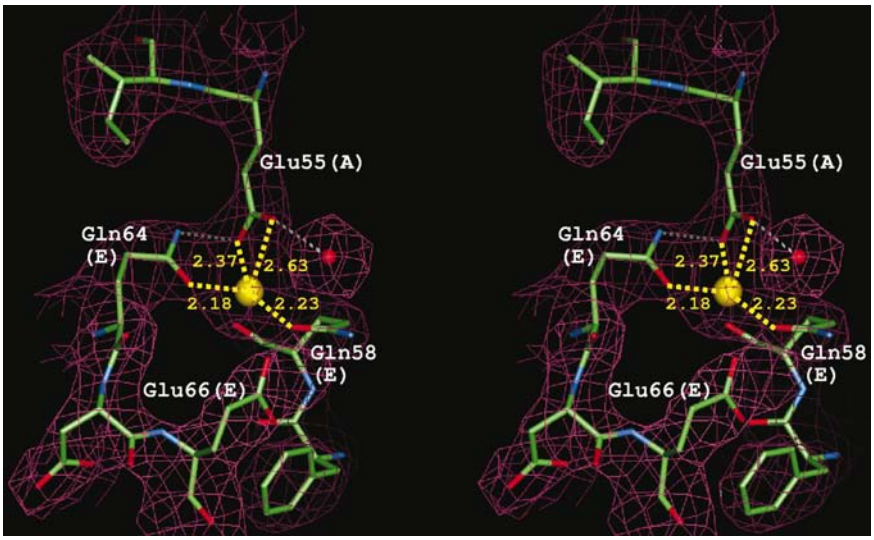

Figure 3
Stereoview of the electron density for the region of the inter-dimer calcium-binding sites overlapped with the final model, with the $2F_o - F_c$ electron-density map contoured at the 1σ level (0.17 e Å^{-3}). Ca^{2+} coordination is shown in yellow dashed lines and the hydrogen bonds are indicated as blue dashed lines. The calcium ion is in yellow and the water molecule is in red. This figure and Fig. 5 were generated using *QUANTA* (Molecular Simulations Inc.).

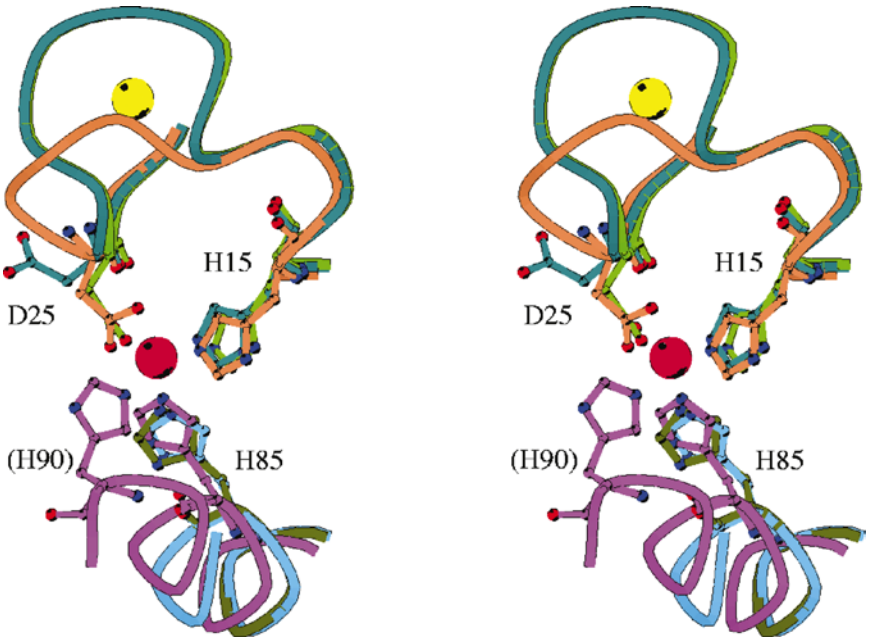

Figure 4
Stereoview of the C^{α} traces of the putative Zn-binding site in S100A12 overlapped with the Zn-binding site in S100A7 (PDB code 2psr). Zn-binding residues are shown in ball-and-stick representation. The 'Zn-open' site in S100A12 is shown in blue and the 'Zn-closed' site is in green (different shades for different subunits); the two subunits of S100A7 are in orange and magenta. The zinc ion is in red.

3.2. Comparison with the *R*3 structure

The most significant differences between the conformations of the residues in the $P2_1$ and *R*3 structures lie in the additional calcium-binding sites. Another unexpected difference is the conformation of the putative Zn^{2+}/Cu^{2+}-binding sites, which had been suggested on the basis of sequence comparisons with S100A7, for which a Zn-bound structure has been published (Brodersen *et al.*, 1999). Comparison of the *R*3 structure of S100A12 with the structure of Zn-bound S100A7 (PDB codes 2psr, 3psr) shows that the putative Zn-binding sites in S100A12 are in a conformation close to that seen in Zn-loaded S100A7, even though they do not contain Zn ions. The situation is different for the hexamer structure presented here, where seven subunits are in the zinc-bound conformation and four (*A*, *F*, *G*, *I*) are in the 'Zn-free' conformation with Glu25 turned away from the Zn-binding site (Fig. 4), while there is no electron density for Glu25 in subunit *L*. It is possible that the open 'Zn-free' conformation is required for S100A12 to be able to incorporate Zn^{2+} (or Cu^{2+}) ions at these unoccupied sites and that the resulting conformational changes might be important for its function. Our attempts to obtain a Zn^{2+}-bound S100A12 structure have not so far been successful, as Zn-containing crystals only diffract to very low resolution. However, we have recently obtained copper containing crystals and our preliminary low-resolution results suggest that Cu^{2+} binds to the predicted Zn^{2+}/Cu^{2+}-binding motif (Moroz, Wilson and Bronstein, unpublished results).

3.3. Location of putative target-binding sites and possible biological implications

Sequence and structure comparison between members of the S100 family have suggested that the target-binding region in dimeric S100A12 is most probably formed by the linker region and the C-terminal residues of one subunit and the N-terminal residues of another subunit, creating two binding sites per dimer (Moroz *et al.*, 2001). These putative binding sites lie on the outer surface of the hexamer (Fig. 5*a*), giving the hexamer the capacity to make multimeric interactions with its receptor, namely the extracellular domains of RAGE. The extracellular calcium concentration is around 1 m*M* or more, which is 10 000-fold greater than inside the cell (Williams, 1996). Such a calcium concentration is sufficient to lead to S100A12 hexamer formation according to DLS analysis. This suggests that the hexameric assembly may be one of the extracellular forms of S100A12, which binds to RAGE.

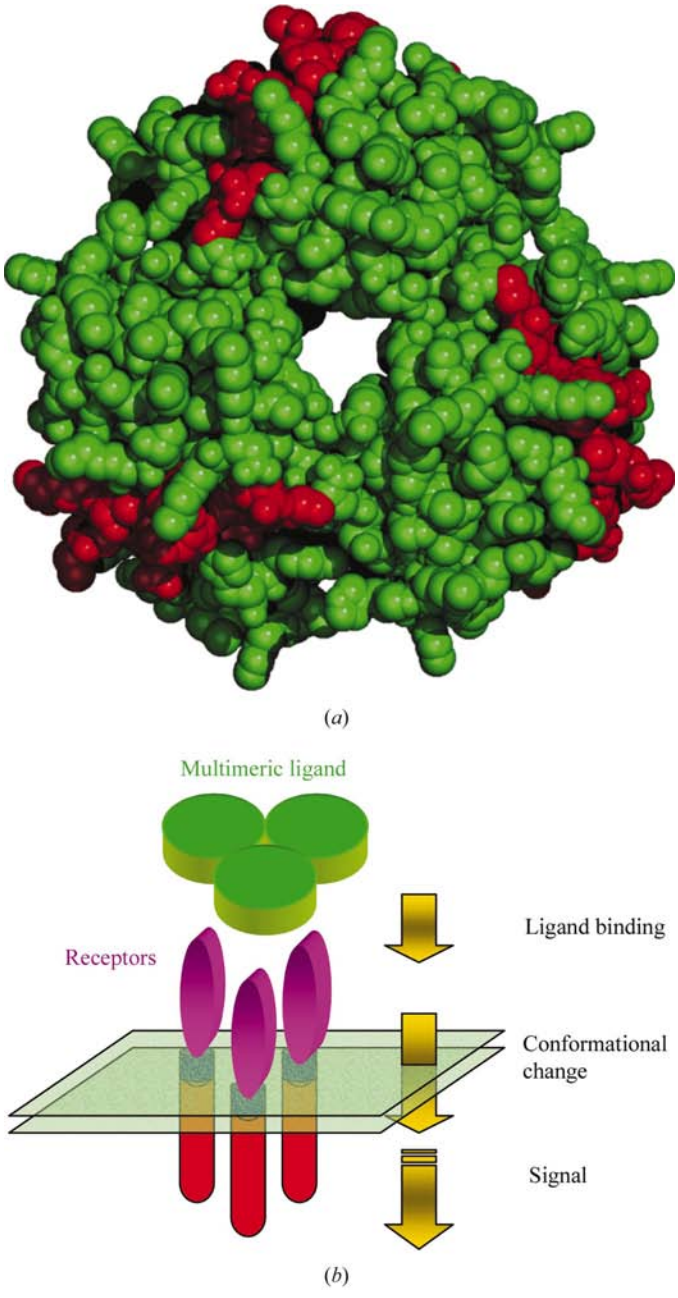

Figure 5
(*a*) Surface representation of the S100A12 hexamer, with the putative target-binding sites (residues 1–11, 40–46 and 79–85) marked in red. (*b*) Scheme illustrating the 'receptor oligomerization' signalling mechanism. The extracellular domains of the receptor are shown in magenta, the transmembrane domains in blue, the cytoplasmic domains in red, the cell membrane in transparent green and the oligomeric ligand in green.

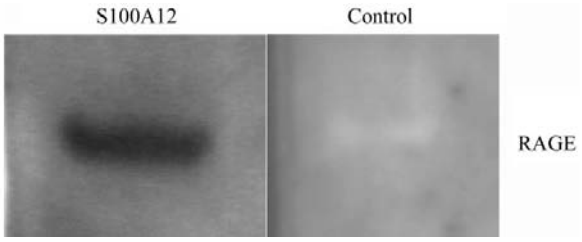

Figure 6
Far-Western blot detecting interaction between RAGE and S100A12. First lane: the membrane was incubated for 1 h at room temperature with S100A12 in blocking buffer. Protein complex was detected by incubation with rabbit polyclonal anti-S100A12 and then with peroxidase-conjugated anti-rabbit IgG antibody. Second lane: the same membrane not incubated with S100A12; all other procedures were the same as for the first lane.

It has been shown that binding of S100A12 to RAGE is a key step in one of the proinflammatory pathways (Hofmann *et al.*, 1999). We have cloned, expressed and purified a fragment of the RAGE extracellular domain and have demonstrated by Far-Western blot analysis that this fragment binds to S100A12 (Fig. 6).

Because there are several lines of evidence that receptor oligomerization is one of the steps in the process of signal transduction, we suggest that by analogy with the activation of TNF superfamily receptors by TNF family cytokines, the S100A12 hexameric assembly interacts with three RAGE extracellular domains to form a complex with trimeric symmetry (Fig. 5*b*). As a result, the cytoplasmic domains of the receptor come into close proximity, inducing intracellular signalling. Thus, the first step of such signal propagation in the extracellular space could be induced by calcium, generating hexamers from the S100A12 dimers, with their six potential Zn/Cu-binding sites possibly involved in receptor activation.

Further experiments and crystal structures of S100–RAGE complexes are certainly required to gain support for our hypothesis. Understanding the atomic interactions of RAGE–S100 complexes will provide the insights essential for understanding the molecular and genetic factors that govern these initial signalling events and provide a structural basis for the design of ligands and the development of potential drugs.

This work was funded by Yorkshire Cancer Research grant No. Y242 and the Danish Cancer Society. We thank the BBSRC for the financial support to the infrastructure of the York Structural Biology Laboratory, contract No. 87/SB09829

(UK). We thank the staff of the ESRF for provision of synchrotron facilities through the block allocation to York.

References

Ambartsumian, N., Klingelhofer, J., Grigorian, M., Christensen, C., Kriajevska, M., Tulchinsky, E., Georgiev, G., Berezin, V., Bock, E., Rygaard, J., Cao, R., Cao, Y. & Lukanidin, E. (2001). *Oncogene*, **20**, 4685–4695.

Banner, D. W., Darcy, A., Janes, W., Gentz, R., Shoenfeld, H. J., Broger, C., Loetscher, H. & Lesslauer, W. (1993). *Cell*, **73**, 431–445.

Bazan, F. (1990). *Proc. Natl Acad. Sci. USA*, **87**, 6934–6938.

Bravo, J. & Heath, J. K. (2000). *EMBO J.* **19**, 2399–2411.

Brodersen, D. E., Nyborg, J. & Kjeldgaard, M. (1999). *Biochemistry*, **38**, 1695–1704.

Collaborative Computational Project, Number 4 (1994). *Acta Cryst.* D**50**, 760–763.

Cowtan, K. (1998). *Acta Cryst.* D**54**, 750–756.

Dell'Angelica, E. C., Schleicher, C. H. & Santome, J. A. (1994). *J. Biol. Chem.* **269**, 28929–28936.

Donato, R. (2001). *Int. J. Biochem. Cell Biol.* **33**, 637–668.

Guignard, F., Mauel, J. & Markett, M. (1995). *Biochem. J.* **309**, 395–401.

Harding, M. M. (2001). *Acta Cryst.* D**57**, 401–411.

Harpaz, Y. & Chothia, C. (1994). *J. Mol. Biol.* **238**, 528–539.

Heizmann, C. W. & Cox, J. A. (1998). *Biometals*, **11**, 383–397.

Hitomi, J., Maruyama, K., Kikuchi, Y., Nagasaki, K. & Yamaguchi, K. (1996). *Biochem. Biophys. Res. Commun.* **228**, 757–763.

Hofmann, M. A., Drury, S., Fu, C., Qu, W., Taguchi, A., Lu, Y., Avila, C., Kambham, N., Bierhaus, A., Nawroth, P., Neurath, M. F., Slattery, T., Beach, D., McClary, J., Nagashima, M., Morser, J., Stern, D. & Schmidt, A. M. (1999). *Cell*, **97**, 889–901.

Hogg, N. (2001). Personal communication.

Huttunen, H. J., Fages, C. & Rauvala, H. (1999). *J. Biol. Chem.* **274**, 19919–19924.

Kligman, D. & Hilt, D. C. (1988). *Trends Biochem. Sci.* **13**, 437–442.

Kraulis, P. (1991). *J. Appl. Cryst.* **24**, 946–950.

Landriscina, M., Bagala, C., Mandinova, A., Soldi, R., Micucci, I., Bellum, S., Prudovsky, I. & Maciag, T. (2001). *J. Biol. Chem.* **276**, 25549–25557.

Landriscina, M., Soldi, R., Bagala, C., Micucci, I., Bellum, S., Tarantini, F., Prudovsky, I. & Maciag, T. (2001). *J. Biol. Chem.* **276**, 22544–22552.

Laskowski, R. A., MacArthur, M. W., Moss, D. S. & Thornton, J. M. (1993). *J. Appl. Cryst.* **26**, 283–291.

Luecke, H., Chang, B. T., Mailliard, W. S., Schlaepfer, D. D. & Haigler, H. T. (1995). *Nature (London)*, **378**, 512–515.

McWhirter, S. M., Pullen, S. S., Holton, J. M., Crute, J. J., Kehry, M. R. & Alber, T. (1999). *Proc. Natl Acad. Sci. USA*, **96**, 8408–8413.

Marti, T., Ertmann, K. D. & Gallin, M. Y. (1996). *Biochem. Biophys. Res. Commun.* **221**, 454–458.

Miranda, L. P., Tao, T., Jones, A., Chernushevich, I., Standing, K. G., Geczy, C. L. & Alewood, P. F. (2001). *FEBS Lett.* **488**, 85–90.

Moroz, O. V., Antson, A. A., Dodson, G. G., Wilson, K. S., Skibshoj, I., Lukanidin, E. M. & Bronstein, I. B. (2000). *Acta Cryst.* D**56**, 189–191.

Moroz, O. V., Antson, A. A., Murshudov, G. N., Maitland, N. J., Dodson, G. G., Wilson, K. S., Skibshøj, I., Lukanidin, E. & Bronstein, I. B. (2001). *Acta Cryst.* D**57**, 20–29.

Murshudov, G. N. & Dodson, E. J. (1997). *CCP4 Newsl. Protein Crystallogr.* **33**, 31–39.

Naismith, J. H., Devine, T. Q., Kohno, T. & Sprang, S. R. (1996). *Structure*, **4**, 1251–1262.

Navaza, J. (1994). *Acta Cryst.* A**50**, 157–163.

Neeper, M., Schmidt, A. M., Brett, J., Yan, S. D., Wang, F., Pan, Y. C. E., Elliston, K., Stern, D. & Shaw, A. (1992). *J. Biol. Chem.* **267**, 14998–15004.

Ni, Ch.-Zh., Welsh, K., Leo, E., Chiou, Ch.-K., Wu, H., Reed, J. C. & Ely, K. R. (2000). *Proc. Natl Acad. Sci. USA*, **97**, 10395–10399.

Nishikawa, T., Lee, I. S. M., Shiraishi, N., Ishikawa, T., Ohta, Y. & Nishikami, M. (1997). *J. Biol. Chem.* **272**, 23037–23041.

Nonato, M. C., Garratt, R. C., Schleicher, C. H., Santome, J. A. & Oliva, G. (1997). *Acta Cryst.* D**53**, 200–202.

Novitskaya, V., Grigorian, M., Kriajevska, M., Tarabykina, S., Bronstein, I., Bock, E. & Lukanidin, E. (2000). *J. Biol. Chem.* **275**, 41278–41286.

Oldfield, T. J. (1994). *Proceedings of the CCP4 Study Weekend. From First Map to Final Model*, edited by S. Bailey, R. Hubbard & D. Waller, pp. 15–18. Warrington: Daresbury Laboratory.

Otwinowski, Z. & Minor, W. (1997). *Methods Enzymol.* **276**, 307–326.

Park, Y. C., Burkitt, V., Villa, A. R., Tong, L. & Wu, H. (1999). *Nature (London)*, **398**, 533–538.

Ramakrishnan, C. & Ramachandran, G. N. (1965). *Biophys. J.* **5**, 909–933.

Robinson, M. J. & Hogg, N. (2000). *Biochem. Biophys. Res. Commun.* **275**, 865–870.

Réty, S., Sopkova, J., Renouard, M., Osterloh, D., Gerke, V., Tabaries, S., Russo-Marie, F. & Lewit-Bentley, A. (1999). *Nature Struct. Biol.* **6**, 89–95.

Schäfer, B. W., Fritscy, J. M., Murmann, P., Troxler, H., Durussel, I., Heizmann, C. W. & Cox, J. A. (2000). *J. Biol. Chem.* **275**, 30623–30630.

Schäfer, B. W. & Heizmann, C. W. (1996). *Trends Biochem. Sci.* **21**, 134–140.

Schomaker, V. & Trueblood, K. N. (1968). *Acta Cryst.* B**24**, 63–76.

Springer, T. (1990). *Nature (London)*, **346**, 425–434.

Strupat, K., Rogniaux, H., Dorsselaer, A. V., Roth, J. & Vogl, T. (2000). *J. Am. Soc. Mass Spectrom.* **11**, 780–788.

Taguchi, A., Blood, D. C., del Toro, G., Canet, A., Lee, D. C., Qu, W., Tanji, N., Lu, Y., Lalla, E., Fu, C., Hofmann, M. A., Kislinger, T., Ingram, M., Lu, A., Tanaka, H., Hori, O., Ogawa, S., Stern, D. M. & Schmidt, A. M. (2000). *Nature (London)*, **405**, 354–360.

Tarabykina, S., Scott, D. J., Herzyk, P., Hill, T. J., Tame, J. R. H., Kriajevska, M., Lafitte, D., Derrick, P. J., Dodson, G. G., Maitland, N. J., Lukanidin, E. M. & Bronstein, I. B. (2001). *J. Biol. Chem.* **276**, 24212–24222.

Thiel, D. J., le Du, M.-H., Walter, R. L., D'Arcy, A., Chene, C., Fountoulakis, M., Garotta, G., Winkler, F. K. & Ealick, S. E. (2000). *Structure*, **8**, 927–936.

Vogl, T., Propper, C., Hartmann, M., Strey, A., Strupat, K., van den Bos, C., Sorg, C. & Roth, J. (1999). *J. Biol. Chem.* **274**, 25291–25296.

Wajant, H., Henkler, F. & Scheurich, P. (2001). *Cell. Signal.* **13**, 389–400.

Whittingham, J. L., Edwards, D. J., Antson, A. A., Clarkson, J. M. & Dodson, G. G. (1998). *Biochemistry*, **37**, 11516–11523.

Williams, R. J. P. (1996). *Cell Calcium*, **20**, 87–93.

Winn, M. D., Isupov, M. & Murshudov, G. N. (2001). *Acta Cryst.* D**57**, 122–133.

Yan, S. D., Chen, X., Fu, J., Chen, M., Zhu, H. J., Roher, A., Slattery, T., Zhao, L., Nagashima, M., Morser, J., Migheli, A., Nawroth, P., Stern, D. & Schmidt, A. M. (1996). *Nature (London)*, **382**, 685–691.

Yang, Z., Tao, T., Raftery, M. J., Youssef, P., Di Girolamo, N. & Geczy, C. L. (2001). *J. Leukocyte Biol.* **69**, 986–994.

Ye, H., Park, Y. C., Kreishman, M., Kieff, E. & Wu, H. (1999). *Mol. Cell*, **4**, 321–330.